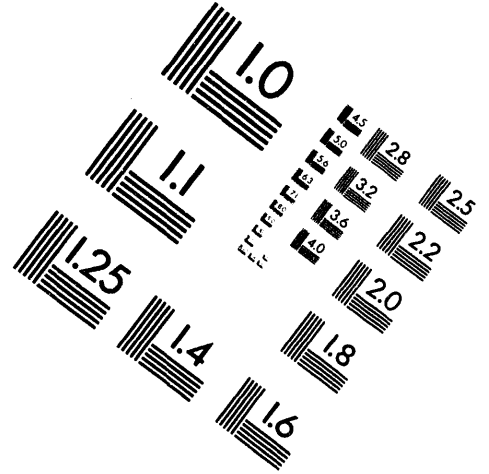
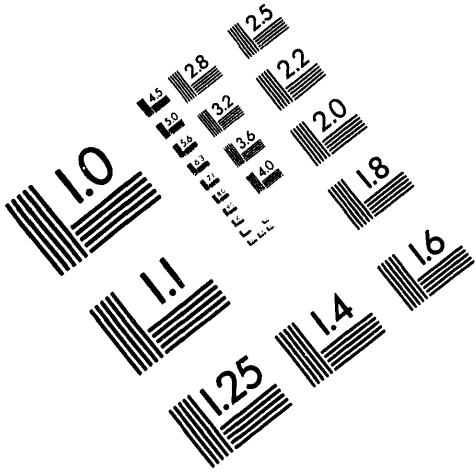




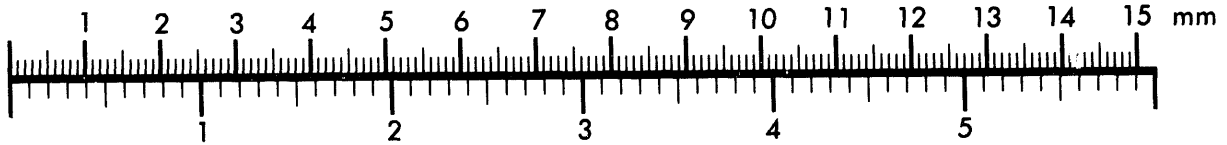
**AIM**

**Association for Information and Image Management**

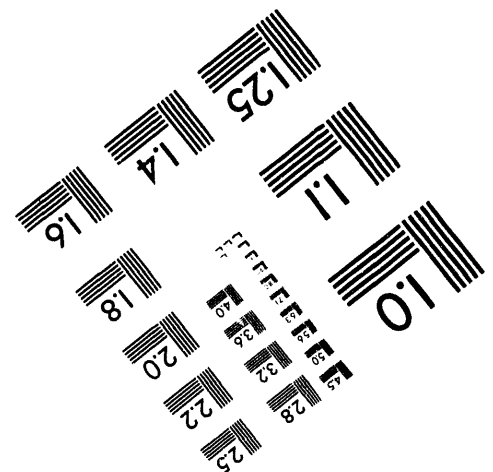
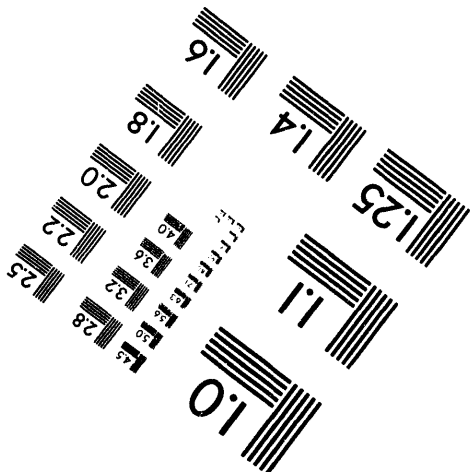
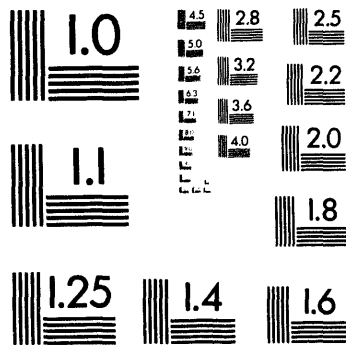
1100 Wayne Avenue, Suite 1100  
Silver Spring, Maryland 20910  
301/587-8202



Centimeter



Inches



MANUFACTURED TO AIM STANDARDS  
BY APPLIED IMAGE, INC.

**1 of 1**

DOE/BC/14852--8

**SCALE-UP OF MISCIBLE FLOOD PROCESSES FOR  
HETEROGENEOUS RESERVOIRS**

**QUARTERLY REPORT  
(APRIL 1 - JUNE 30, 1994)**

**Franklin M. Orr, Jr.  
Principal Investigator**

**Department of Petroleum Engineering  
Stanford University  
Stanford, California 94305-2220**

**Prepared for the U.S. Department of Energy  
Under Grant No. DE-FG22-92BC14852**

**July 1994**

"US/DOE Patent Clearance is not required prior to the publication of this document."

**DISCLAIMER**

This report was prepared as an account of work sponsored by an agency of the United States Government. Neither the United States Government nor any agency thereof, nor any of their employees, makes any warranty, express or implied, or assumes any legal liability or responsibility for the accuracy, completeness, or usefulness of any information, apparatus, product, or process disclosed, or represents that its use would not infringe privately owned rights. Reference herein to any specific commercial product, process, or service by trade name, trademark, manufacturer, or otherwise does not necessarily constitute or imply its endorsement, recommendation, or favoring by the United States Government or any agency thereof. The views and opinions of authors expressed herein do not necessarily state or reflect those of the United States Government or any agency thereof.

RECEIVED  
USDOE/PETC  
94 JUL 25 PM 2:40  
ADMINISTRATIVE

**MASTER**

DISTRIBUTION OF THIS DOCUMENT IS UNLIMITED *JFD*

# 1 Introduction

The current project is a systematic research effort to quantify relationships between process mechanisms that can lead to improved recovery from gas injection processes performed in heterogeneous Class 1 and Class 2 reservoirs. It will provide a rational basis for the design of displacement processes that take advantage of crossflow due to capillary, gravity and viscous forces to offset partially the adverse effects of heterogeneity. In effect, the high permeability zones are used to deliver fluid by crossflow to zones that would otherwise be flooded only very slowly. Thus, the research effort is divided into five areas:

- Development of miscibility in multicomponent systems
- Design estimates for nearly miscible displacements
- Design of miscible floods for fractured reservoirs
- Compositional flow visualization experiments
- Simulation of near-miscible flow in heterogeneous systems

The status of the research effort in each area is reviewed briefly in the following section.

## 2 Project Status

### • Development of Miscibility in Multicomponent Systems

We are making progress on the creation of a systematic theory of miscibility development in multicomponent systems. The dispersion-free theory developed previously at Stanford shows that in any multicomponent displacement, the recovery behavior is determined by a small number of key tie lines that include the tie lines that extend through the initial and injection compositions, and one or more crossover tie lines. If any of those tie lines is a critical tie line, then the displacement is multicontact miscible. Thus the key to determining minimum miscibility pressure (or minimum enrichment for miscibility) is to find which tie line approaches the critical locus first as pressure (or enrichment) is increased. Graduate student Bruno Aleonard is currently investigating efficient algorithms for calculation of the critical locus. The next step is to develop an algorithm to determine which tie line lies closest to the critical locus. Once the key tie line for miscibility is so identified, it should be possible to develop an efficient algorithm to determine minimum miscibility pressure for a multicomponent system. Ph.D. student Yun Wang has joined the research group to work on theory for systems with more than four components. Our goal is to develop a mathematical technique that will allow to solve dispersion-free flow problems for systems with an arbitrary number of components.

### • Design Estimates for Nearly Miscible Displacements

The scaling theory developed last year has been extended to include the effects of layer ordering in scaling nearly miscible displacements in layered reservoirs. We found, as others

have, that gravity forces can offset the adverse effects of high permeability channels in some layered reservoirs if adequate vertical communication exists, a result that agrees with observations obtained in our visualization experiments [33].

We have also investigated the effects of gravity and viscous forces on residual oil saturations. Our flow models and experimental results showed that gravity and viscous forces are additive in determining residual oil saturations. For systems in which gravity and viscous forces are comparable, gravity favorable displacements result in much less residual oil saturation than do the gravity unfavorable displacements. The directional effects of gravity forces on residual oil saturation show that gravity forces can improve the residual oil saturation, as well as the macroscopic sweep efficiency [33].

- **Design of Miscible Floods for Fractured Reservoirs**

We have finished our first stage of modifying the existing high pressure PVT equipment to conduct high pressure gravity drainage experiments. In the first experiment, now underway, we used Means crude, whose phase behavior with CO<sub>2</sub> has been well studied in our laboratory [12]. A 2-ft long and 2.5-in diameter sandstone core was saturated with 0.73 pore volume (PV) of crude oil and 0.27 PV of water, before it was surrounded with liquid CO<sub>2</sub> at 900 psi and room temperature (about 22°C). Preliminary results show that significant gravity drainage occurs even at fairly low pressure (900 psi). We are in the process of systematically studying gravity drainage in a pressure range from 900 psi to 1500 psi, in order to investigate the effects of miscibility development and consequent changes in interfacial tension on gravity drainage rates and final oil recovery.

In this area, we have also made progress in developing a theory of three phase gravity drainage. Recent experimental and theoretical results suggest that we can obtain zero residual oil saturation in some parts of a reservoir, if the reservoir is water-wet and the system has a positive spreading coefficient [4]. Those results are reported in detail in the research result section below.

- **Flow Visualization Experiments**

To understand more fully the visualization experimental results we have obtained, we are in the process of modifying a compositional simulator code to simulate the experiments. A subroutine for calculating the phase behavior of the fluid system used in our experiments has been written. The oil-water-alcohol systems used in the low pressure experiments are not modeled accurately by cubic equations of state, and hence an approach based on excess free energy models is being used.

- **Simulation of Flow in Heterogeneous Reservoirs**

We have continued to investigate the streamtube approach as a numerical alternative to conventional finite difference simulators to be used in predicting near-miscible gas injection in heterogeneous reservoirs. We have tested our technique on ideal miscible and two phase, multicomponent displacements and showed that the Riemann technique is accurate and reduced computation time compared to conventional simulation by two to three orders of magnitude [29].

Because the one-dimensional solution may be calculated analytically or numerically using a large number of blocks, numerical diffusion is completely absent or minimized. Mapping such a one-dimensional solution along streamtubes automatically eliminates the problem of numerical diffusion and permits investigation of the interaction of phase behavior, reservoir heterogeneity, and nonlinearity [29].

## 3 Research Results

In this section, we report in detail our recent results from a study of three phase flow and gravity drainage in porous media. This study was conducted by Research Associate Dengen Zhou, Ph.D. student Darryl Fenwick and Prof. Martin Blunt.

### 3.1 Introduction

The displacement of oil by gas in the presence of water is an important recovery process in oil fields and in the cleanup of contaminants spilled below ground. The displacement of oil by gas under gravity (gravity drainage) occurs in oil reservoirs when the gas cap expands as the pressure drops, when oil condensate forms, or when gas is injected into the gas cap. Three phase flow is also seen when natural gas, nitrogen, carbon dioxide or steam are injected into the field to displace oil. In an environmental context, the spilling and leakage of hydrocarbons and organic solvents are major contributors to groundwater contamination. The low solubility of these products means that they are often present in their own phase. An oil that is less dense than water, such as a fuel, will migrate downwards until it rests above the water table. The effects of water table movement, capillarity and gravity will smear the oil in a region above and below the water table, where both air and water are also present. Artificial lowering of the water table by pumping results in the displacement of oil by air through a wet soil. This again is a gravity drainage process. Since the work of Dumore and Schols [10], it has been known that gravity drainage in water-wet rock can lead to a high oil recovery, with residual oil saturations of a few percent in the presence of immiscible gas and water, which is much lower than the residual oil saturation in the presence of water alone. Further studies on sandstone cores, bead packs and sand columns [6, 16, 31] confirmed these results. It was suspected that the high oil recovery was due to drainage through films of oil that lie between the water and the gas in the pore space. This film drainage has been observed directly in two dimensional etched glass micromodels by Kantzas et al. [17], Oren et al. [24], Oren and Pinczewski [23], Kalaydjian [14] and Soll et al. [28]. It was shown by Oren et al. [24], Vizika [31] and Kalaydjian [15] that systems with a positive spreading coefficient, which means that the oil spontaneously spreads over a water/gas interface, would experience film drainage and high recoveries, whereas nonspreading systems would see lower recoveries. It was suggested by Kantzas et al. [17] that the recovery could be determined by the stability of the oil film, which is controlled by capillary and intermolecular forces, rather than the spreading coefficient alone. In this work, we investigated the fundamental mechanisms of oil recovery in three phase flow, in water-wet porous media, starting at the molecular scale, and provides a predictive theory of gravity drainage. The principal issues are: (1) the thickness and stability of thin oil films controlled by intermolecular forces; (2) the thickness of oil layers during

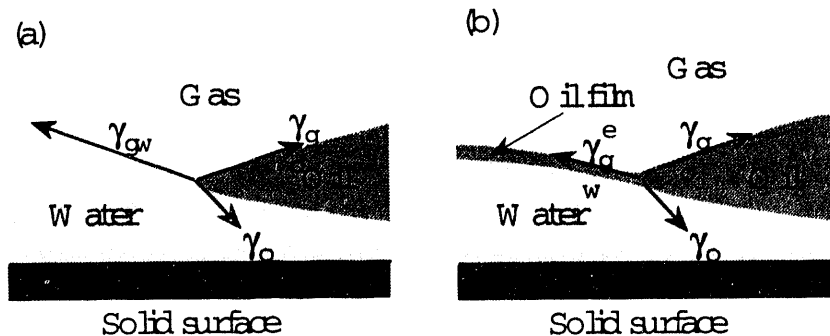


Figure 1: Distributions of three fluids in contact. (A) when  $C_s > 0$ ; and (B) when  $C_s < 0$ .

drainage; (3) the flow rate in these layers; (4) the final oil recovery and fluid distribution. We will show that for a spreading system (typical of most fluids in polluted soil and oil reservoirs), the oil layer provides pressure continuity for the oil phase, thus preventing it from being trapped. Oil can drain rapidly by swelling these layers to occupy the crevices and roughness in the pore space. However, the final oil saturation can be essentially zero, with the oil confined to thin, molecular films. In vertical capillary/gravity equilibrium, where the oil density is less than that of water, there is a finite height above the water table (or the water/oil contact) where the connected oil saturation is zero. This height is determined solely by the height of the oil bank, and the surface tensions and densities of the fluids, but is independent of the pore size distribution. Non-spreading systems do not allow drainage of oil layers and give lower recoveries from gravity drainage. These findings are confirmed by a series of experiments on sand columns and capillary tubes.

### 3.2 Does Oil Spread on Water?

With three phases present in a porous medium, it is possible for oil to spread between water and gas in the pore space. This phenomenon is determined by the spreading coefficient  $C_s$ ,

$$C_s = \gamma_{gw} - \gamma_{go} - \gamma_{ow}, \quad (1)$$

where  $\gamma_{gw}$ ,  $\gamma_{go}$  and  $\gamma_{ow}$  are the gas/water, gas/oil and oil/water surface tensions respectively measured on the fluids before they are brought into contact with each other. If  $C_s > 0$ , the contact line between the three phases is unstable and the oil spreads, as shown in Fig. 1. Most solvents, hydrocarbons and crude oils (see p. 104, Table 5 of [21]) do have a positive spreading coefficient.

In this work we will distinguish between an oil film, a few nanometers across, and an oil layer which may occupy crevices in the pore space and be microns thick. On a flat substrate, the oil eventually forms a film of approximately molecular thickness, between 0.5 and 5 nm across. This behavior is consistent with everyday experience: gasoline spilled on a puddle of

water, for instance, will spread until it forms a thin, iridescent film on the water that is only of order a molecular diameter across. The water/gas interface containing this oil film has a much lowered effective surface tension for which, if there is no pressure difference across the film, the effective spreading coefficient is zero or negative [1, 11, 27]. The thickness of an oil film can be predicted by calculating the van der Waals forces between the water, oil and gas. Our computation of the film thickness is similar to the work of Oren and Pinczewski [22], although we use the complete expression for the van der Waals force [3]. We have shown [4] that on a flat surface most hydrocarbons form a film, whose thickness depends on the capillary pressure and displacement history. The same behavior has been predicted for wetting films [13]. The film provides pressure continuity for the oil phase. This means that isolated oil ganglia, trapped and surrounded by water, can become connected during gas injection, when the gas contacts the oil. However, we will show that the drainage rate through these films is far too slow to account for the oil recoveries observed experimentally. Thicker oil layers in crevices of the pore space must provide channels for more rapid drainage.

### 3.3 Configuration of Three Phases in the Pore Space

#### Oil films in a cylinder

Fig. 2 shows the schematic arrangement of fluid in a cylindrical concavity of the pore space. Water wets the solid. Oil is intermediate-wet and occupies a film of thickness  $t$ , while the gas, being nonwetting, fills the center of the cylinder. The equilibrium film thickness is found from the augmented Young-Laplace equation

$$P_{cgo} = \Pi_o(t) + \frac{\gamma_{go}}{r - t - w} = \Pi_o(t) + \frac{\gamma_{go}}{r_{go}}, \quad (2)$$

where  $P_{cgo}$  is the gas/oil capillary pressure,  $w$  is the water film thickness,  $r_{go}$  is the radius of curvature of the gas/oil interface and  $\Pi_o(t)$  is the disjoining pressure that accounts for the influence of intermolecular forces on the oil [8]. A positive disjoining pressure is equivalent to a repulsion between the gas and the water, leading to swelling of the oil film, whereas  $\Pi_o(t) < 0$  corresponds to an attractive force that makes the film thinner. At distances greater than a few molecular diameters, the main contribution to the disjoining pressure comes from the dispersive, van der Waals force, which gives a small positive  $\Pi_o(t)$  for  $t$  greater than approximately 10 nm for most alkanes. For  $t$  less than around 10 nm, the intermolecular forces are controlled by steric forces, can be very large and are significant compared with the curvature term in Eq. 2. A similar expression can be written for the pressure difference between the oil and water phases

$$\Pi_{cow} = \Pi_w(w) + \frac{\gamma_{ow}}{r_{ow}}, \quad (3)$$

where  $\Pi_w(w)$  is the disjoining pressure of the water film. Fig. 3 shows  $\Pi_o(t) + \gamma_{go}/r_{go}$  plotted as a function of  $t$  for an n-octane/water/gas system with a representative water film thickness of 10 nm on a quartz capillary of radius 500  $\mu\text{m}$ . The computation of  $\Pi_o(t)$  is described in our previous work [3] and is accurate if  $r_{go} \gg t$ . For  $t$  less than 10 nm, the intermolecular forces are most significant, whereas when  $t$  becomes close to  $r - w$ , the second term in Eq. 2 diverges.

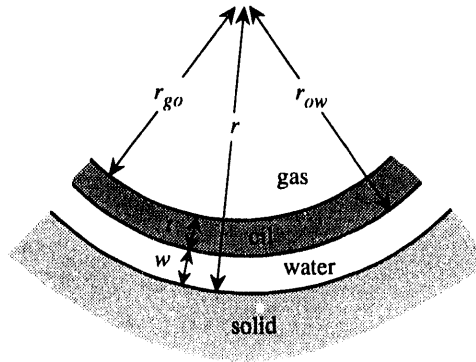


Figure 2: Distribution of three fluids in a cylindrical region of the pore space.

Stable solutions are found when both Eq. 2 is obeyed and  $dP_{cgo}/dt < 0$ . As indicated in Fig. 3, there is a narrow range of capillary pressures, just above  $\gamma_{go}/r_{go}$ , for which a film of thickness between 24 nm and 242 nm is stable, due to the long-range influence of van der Waals forces. At higher capillary pressures, the film collapses to molecular thickness. Such thin films are also observed on convex (protruding) surfaces. If we lower the capillary pressure below  $\gamma_{go}/r_{go}$ , there is no stable solution unless the oil occupies the whole of the cylindrical cross-section and there is no gas present. This spontaneous filling of a pore throat is similar to the snap-off mechanism, which has been described before [20, 26]. The maximum oil film thickness on a cylindrical concavity can be 100s of nanometers. While this is much thicker than a molecular film, it is still more than three orders of magnitude smaller than the radius of curvature of the solid surface.

### Oil layers in an angular crevice

Fig. 4 shows the distribution of oil, water and gas in a square crevice. From geometrical considerations, an oil layer is present if  $r_{go} \geq r_{ow}$ . From the augmented Young-Laplace Eqs. 2 and 3 this means that

$$\frac{P_{cow} - \Pi_w}{\gamma_{ow}} \geq \frac{P_{cgo} - \Pi_o}{\gamma_{go}}. \quad (4)$$

If we consider thick oil layers, with  $w$  and  $t$  taken to be 100 nm or more, the disjoining pressures will be negligible, in which case the inequality above reduces to

$$\frac{P_{cow}}{\gamma_{ow}} \geq \frac{P_{cgo}}{\gamma_{go}}. \quad (5)$$

If the oil/water pressure difference is much larger than the gas/oil pressure difference, it is possible for a thick oil layer to occupy most of the crevice. A large oil/water capillary pressure forces the water into the corner, while a relatively low gas/oil capillary pressure allows a thick oil layer to develop. This can be true for any angular or sharp groove in the pore space. Since pore sizes are typically in the range of 1  $\mu\text{m}$  to 100  $\mu\text{m}$  or more, oil layers several microns across

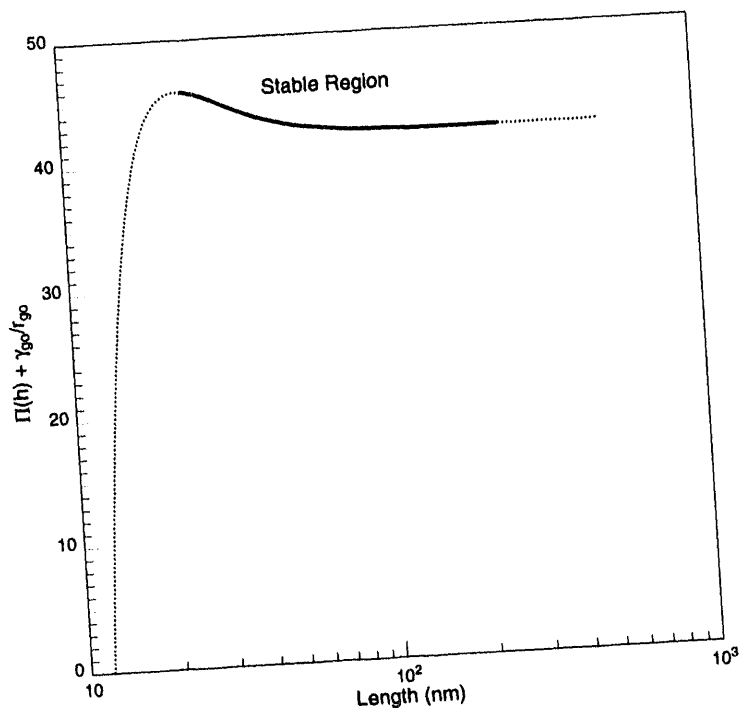


Figure 3:  $\Pi_o(t) + \gamma_{go}/r_{go}$  computed as a function of oil film thickness,  $t$ , using the van der Waals intermolecular force.

can exist. If, however, the inequality (Eq. 5), is not obeyed, only a film of molecular thickness will be stable, where the disjoining pressures in Eq. 4 become significant.

To recap: on locally flat or convex portions of the pore space, the oil film thickness is a few nanometers; a cylindrical concavity, with a radius of several 100 microns, can support films tens to hundreds of nanometers across; whereas for sharp or angular crevices, layers several microns thick will form if the oil/water capillary pressure is much larger than the gas/oil capillary pressure. If the spreading coefficient is negative, a three phase contact line is stable, as shown in Fig. 1, and no oil films are seen.

### 3.4 Drainage Rates

#### Predicted rates

Fig. 5 shows the vertical arrangement of water, oil and air (gas) in a capillary tube. There are two oil ganglia separated by an air bubble of height  $h$ . If there is a film of oil that connects the two blobs, there will be pressure continuity in the oil phase which allows the upper ganglion to drain into the lower one under gravity. Since the air has a low density, the pressures in the two ganglia are approximately equal when drainage starts. The gas/oil interfaces at  $z = 0$  and  $z = h$  are hemispherical caps of radius  $r$ , with a total curvature of  $2/r$ . Thus the gas/oil capillary pressure is approximately  $2\gamma_{go}/r$ . In a capillary tube of square cross-section, the fluid configuration is shown in Fig. 4. If  $P_{cgo} = 2\gamma_{go}/r$ , then the gas/oil radius of curvature,  $r_{go} = r/2$ . Water will also occupy the corner, but as we increase  $z$ , the oil/water capillary pressure will rise,

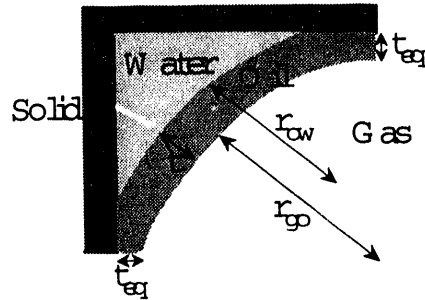


Figure 4: The arrangement of water, oil and gas in a square crevice.

forcing water further into the corner. Thus, for large values of  $h$ , the oil can occupy almost all the corner of the tube, resulting in rapid drainage. For smaller values of  $h$ , the water occupies more of the corners and the drainage rate is lower. The calculation of drainage rates in capillaries of square and circular cross-section was reported in our previous work [32].

Despite its simple geometry, the analysis for a cylindrical capillary is less straightforward. There is no obvious force balance on the oil film and the oil pressure is not easily determined.  $P_{cgo} = 2\gamma_{go}/r$  implies a thin, molecular film and a negligible drainage rate. However, when the tube is held upright, gravity forces instantaneously lead to an increase in oil pressure. Moreover, small vibrations can perturb the pressure in the oil and gas phases.  $\gamma_{go}/r$  is only 42 Pa in the experiments we perform, compared with the atmospheric pressure of  $10^5$  Pa. To match the experimental results below, it appears that the oil pressure rises to make  $P_{cgo} \approx \gamma_{go}/r$  and the oil film swells to reach its maximum stable thickness.

### Experimental confirmation

We tested our predictions for the drainage times by performing a series of experiments with glass capillary tubes. We first filled the tube with water. Then oil was introduced into the tube at one end to form the lower oil ganglion ( $h_2 = 0$ ) this step was omitted. Water was subsequently drained out of the opposite end to allow air to enter the tube. By controlling the amount of water that drained out, we controlled the height of the gas bubble,  $h$ . The last step was to allow some oil into the tube, above the gas. The tube was then placed vertically and we recorded the time for all the oil in the upper ganglion to drain. We conducted experiments for high (iso-octane and distilled water) and low (a mixture of iso-octane, water and iso-propanol partitioned into two phases) oil/water surface tensions. The fluid properties are shown in Table 1. For a capillary tube of circular cross-section with  $r = 500 \mu\text{m}$ ,  $h_2 = 0$  and  $h = 2 \text{ cm}$ , it took three weeks to drain  $0.8 \text{ mm}^3$  of iso-octane from the upper ganglion. The uncertainty in our measurement of the oil volume was  $0.4 \text{ mm}^3$ . This is the same system for which we performed the intermolecular force calculation in the previous section. An oil film of thickness  $t=310 \text{ nm}$  would give this drainage rate. Our predicted oil film thickness from the

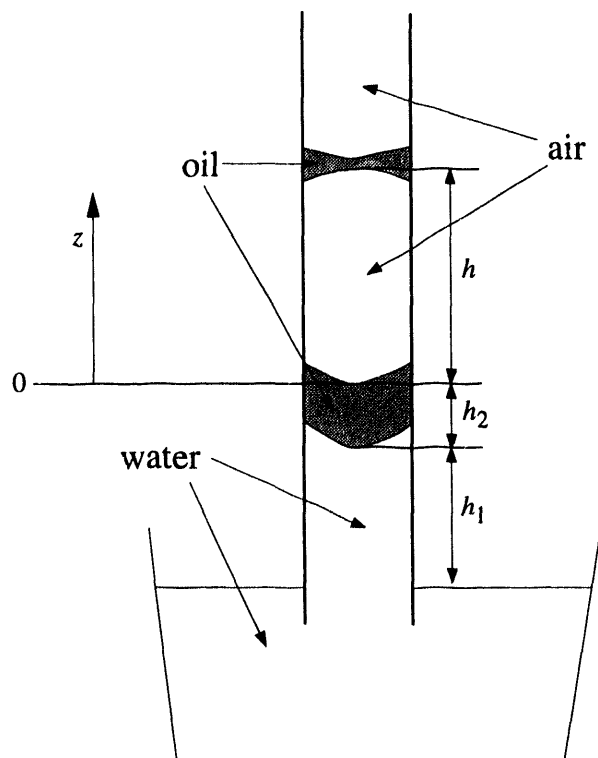


Figure 5: Fluid configuration in a capillary tube at the beginning of drainage.

previous section is 242 nm, which is consistent with our measurements.

We then performed a series of experiments in a capillary tube of square cross-section with a side of length  $150 \mu\text{m}$ . We repeated the experiment for various values of  $h_2$  and  $h$ . In each experiment the volume of oil above the gas was  $0.225 \text{ mm}^3$ .

Fig. 6 shows the results for the system with a high interfacial tension (IFT). The triangles are the drainage times for different values of  $h$  when there is no initial oil bank ( $h_2 = 0$ ) and the squares are the drainage times for the same fluids for various  $h$  and  $h_2 = 4 \text{ cm}$ . Increasing  $h$  reduces the drainage time. The solid and dotted curves are our predicted times. The only unknown parameter in the prediction is the conductance constant for the oil layer. This was estimated to match the experimental results - only one parameter was used to match both curves. The agreement between experiment and theory is good. Notice that the minimum

Table 1: Fluid properties for the experiments presented

Experiments	$\gamma_{ow}(\text{mN/m})$	$\rho_w - \rho_o(\text{kg/m}^3)$	$\rho_o(\text{kg/m}^3)$	$\mu_o(\text{kg}/(\text{ms}))$	$\alpha$
Mineral oil	54	157	833	0.005	8.9
Fig. 6	38.1	310	690	0.00048	4.03
Fig. 7	4.41	305	690	0.00049	0.47

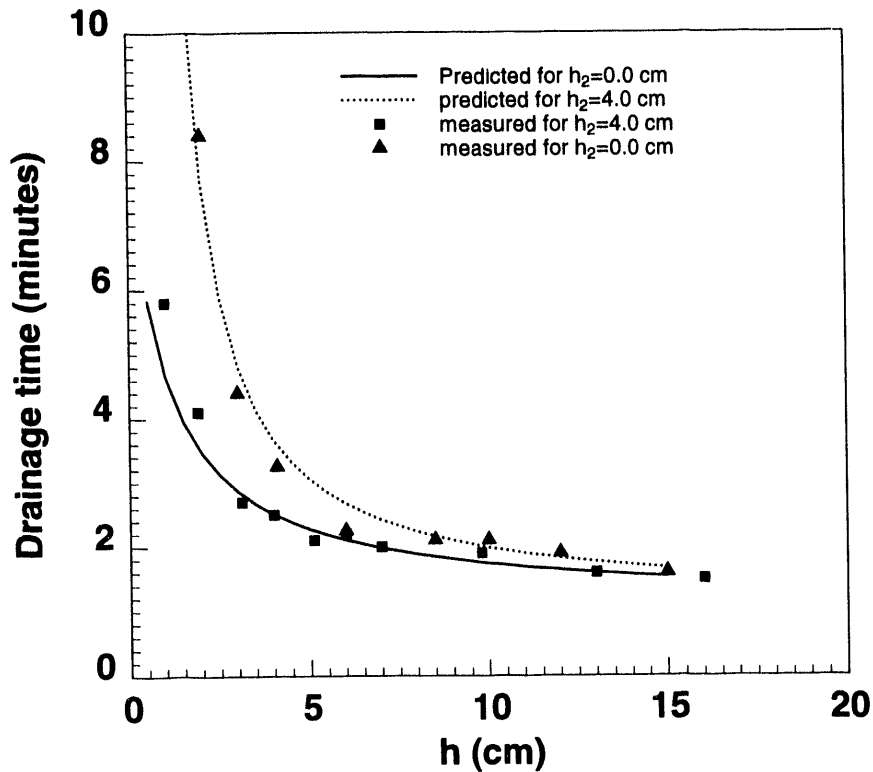


Figure 6: Comparison of measured and predicted drainage times in a capillary tube of square cross-section for a system with a high oil/water surface tension.

drainage time is just a few minutes, or several thousand times faster than in the capillary tube, even though the tube is smaller for this experiment. The reason for this is that the oil can form a much thicker layer (up to  $15 \mu\text{m}$  across) in the corners of the tube than can be supported on a smooth, concave interface (only around 200-300 nm).

Fig. 7 shows the results from the low IFT system in the same capillary tube. Again the agreement between experiment and theory is good. The drainage times are longer because the viscosities of the water and oil phases are higher than for the high IFT fluids. We performed the same experiments with a mineral oil that has a negative spreading coefficient. In this case there was no drainage of the oil, since a spreading film was never established. On square capillaries with a side of 1 mm or larger, droplets of the oil were observed to fall down the glass, like rain droplets on a window pane. However, this phenomenon is only seen for large droplets and large capillaries and is unlikely to be significant in porous media. Real porous media do contain angular or sharp crevices that can support thick oil layers of order microns across during gravity drainage. This provides a mechanism for relatively rapid displacement of oil. Flow rates across flat surfaces or on uniformly concave interfaces are much slower. In all cases there is agreement between the predicted and measured flow rates.

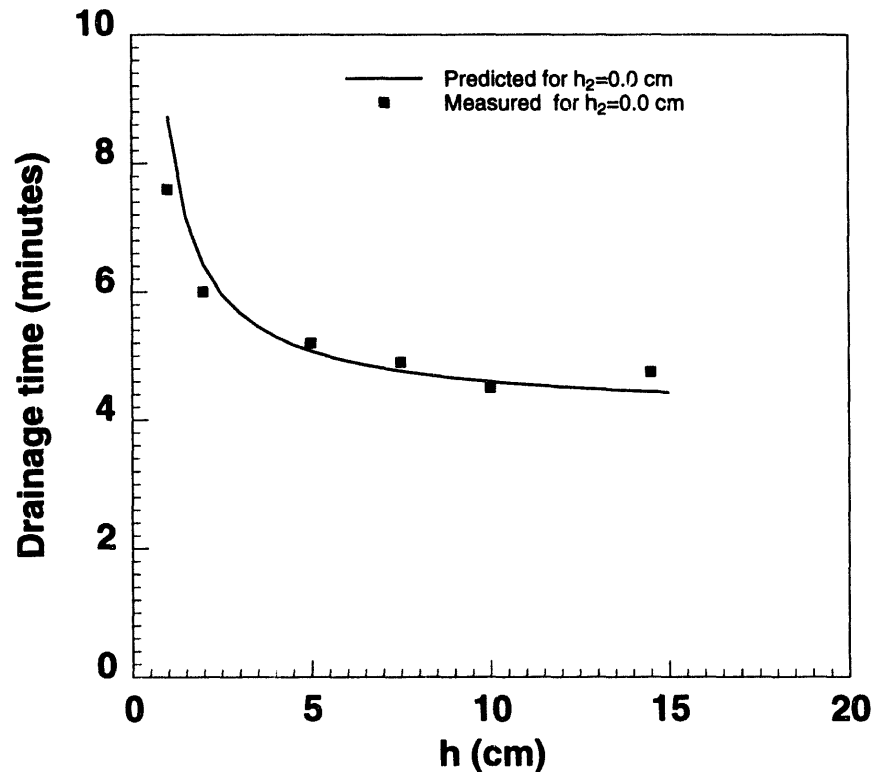


Figure 7: Comparison of measured and predicted drainage times in a capillary tube of square cross-section for a system with a low oil/water surface tension.

### 3.5 Vertical Equilibrium

#### A critical height

We will now analyze the fluid distribution in vertical capillary/gravity equilibrium, at the end of drainage, for systems with a positive spreading coefficient and for oils less dense than water. Consider again the arrangement of fluid illustrated in Fig. 4. Since there is no direct contact of water by gas, to the gas phase, oil and water combined appear to be the wetting phase. This means that the gas/oil capillary pressure can be represented as a function of total liquid saturation ( $S_o + S_w$ ), as first suggested by Leverett [19] and confirmed by Parker et al. [25]. In contrast, when  $C_s < 0$ , oil remains in the system as lenses and is influenced by both oil and water separately. As shown by Kalaydjian [14], this results in a gas/oil capillary pressure that is a function of both  $S_w$  and  $S_o$  rather than  $S_o + S_w$  alone.

Fig. 8 shows gas, oil and water in vertical equilibrium.  $z = 0$  is defined as the level at which oil is first mobile, or continuous, through the soil or rock.  $z = H$  corresponds to the height at which gas is first continuous. Above  $z = H$  all three phases may be continuous. This diagram corresponds to the arrangement of nonaqueous phase pollutant resting on the water table, or oil and gas in a reservoir. Where the phases are connected we can write down expressions for

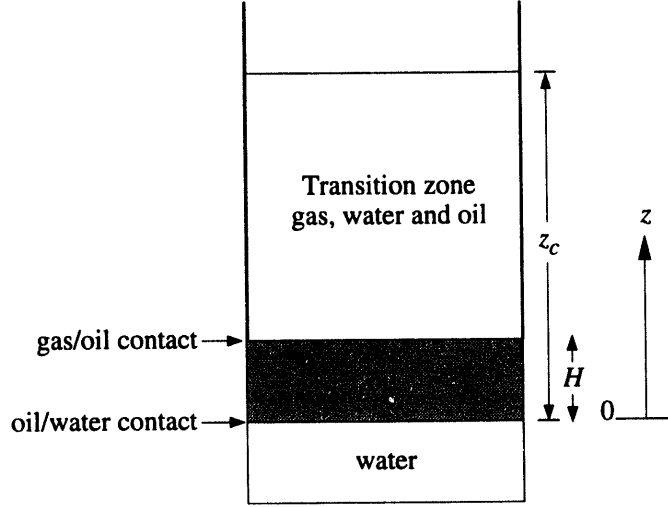


Figure 8: A schematic of the arrangement of water, oil and gas in vertical equilibrium.

the pressures as a function of height

$$P_w = -z\rho_w g, \quad (6)$$

where  $P_w$  is the water pressure,  $g$  the acceleration due to gravity and we define  $P_w = 0$  at  $z = 0$ . Similarly we may write

$$P_o = P_{cow}^* - z\rho_o g, \quad (7)$$

$$P_g = P_{cgo}^* + P_{cow}^* - H\rho_o g - (z - H)\rho_g g, \quad (8)$$

where  $P_{cow}^*$  and  $P_{cgo}^*$  are the threshold capillary pressures for oil invasion into water and gas invasion into oil respectively. The capillary pressures are

$$P_{cow} = P_o - P_w = P_{cow}^* + z(\rho_w - \rho_o)g, \quad (9)$$

$$P_{cgo} = P_g - P_o = P_{cgo}^* + (z - H)(\rho_o - \rho_g)g. \quad (10)$$

If the spreading coefficient is positive, the gas/oil capillary pressure is a function of the sum of the water and oil saturations. The oil/water capillary pressure, where water is the wetting phase, is a function of  $S_w$ . We assume that the functional forms of both capillary pressures are the same, but multiplied by their respective surface tensions, which control the relative strength of capillary forces [2, 19].

$$P_{cow} = \gamma_{ow}J(s_w) + \Pi_w, \quad (11)$$

$$P_{cgo} = \gamma_{go}J(s_w + s_o) + \Pi_o, \quad (12)$$

where  $J$  is a capillary pressure function that represents the curvature of the fluid interfaces as a function of saturation. In terms of the microscopic configuration of fluid, shown in Fig. 4,

$J(S_w)$  in Eq. 11 is  $1/r_{ow}$  and  $J(S_w + S_o)$  is  $1/r_{go}$ . However, this argument is completely general and does not rely on any particular model of the pore level fluid distribution. The threshold capillary pressures can be written  $P^*_{cow} = \gamma_{ow}J^*$  and  $P^*_{cgo} = \gamma_{go}J^*$ , where  $J^*$  is the curvature necessary for a phase to first enter the porous medium. The capillary pressure decreases with wetting phase saturation [2]. Hence

$$J(S_w) \geq J(S_w + S_o). \quad (13)$$

This is equivalent to stating that  $r_{go} \geq r_{ow}$  for an oil layer to exist in Fig. 4. From Eqs. 11 and 12 the inequality above becomes

$$\frac{P_{cow} - \Pi_w}{\gamma_{ow}} \geq \frac{P_{cgo} - \Pi_o}{\gamma_{go}}. \quad (14)$$

Notice that this is identical to Eq. 4. By using a capillary pressure analysis, or by considering the microscopic arrangement of fluid in a pore, we arrive at the same inequality for continuity of the oil phase. We substitute Eqs. 9 and 10 into 14 to find

$$\frac{z - \frac{\Pi_w}{(\rho_o - \rho_g)g}}{(z - H) - \frac{\Pi_o}{(\rho_w - \rho_o)g}} \geq \alpha, \quad (15)$$

where

$$\alpha = \frac{\gamma_{ow} \rho_o - \rho_g}{\gamma_{go} \rho_w - \rho_o}, \quad (16)$$

$\alpha$  is a property of the fluid surface tensions and densities. This expression, without accounting for disjoining pressure, was first derived by Kantzas et al. [17]. For a bulk phase to be present, the disjoining pressures will be negligible and we may write

$$\frac{z}{z - H} \geq \alpha. \quad (17)$$

For  $0 < \alpha < 1$ , the inequality above is always obeyed, which means that connected oil exists at all heights above the oil bank. If  $\alpha > 1$ , there is a finite height at which oil in thick layers cannot exist, which means that oil must reside in thin films a few nanometers across, where the disjoining pressures are significant. The oil saturation of this film will be at most 0.01% and may be considered negligible. The critical height  $z_c$  at which the oil saturation becomes virtually zero is

$$z_c = \frac{\alpha H}{\alpha - 1} = H + \frac{H}{\alpha - 1}. \quad (18)$$

For systems with  $\alpha > 1$  the minimum oil saturation is zero. In contrast, residual oil saturations in the range 0.1 to 0.5 are encountered in water-saturated porous media [9]. Lowering the water table in a region polluted by free product, or gas cap expansion into a waterflooded reservoir, will mobilize this trapped oil and allow some of it to be recovered by direct pumping.

Fig. 9 shows schematic graphs of saturation versus height for different values of  $\alpha$ . Fig. 9(c), for  $\alpha > 1$ , demonstrates how the connected oil saturation decreases to zero at some critical height  $z_c$ . Above  $z_c$ , the fluid distribution is governed by the gas/water capillary pressure (the

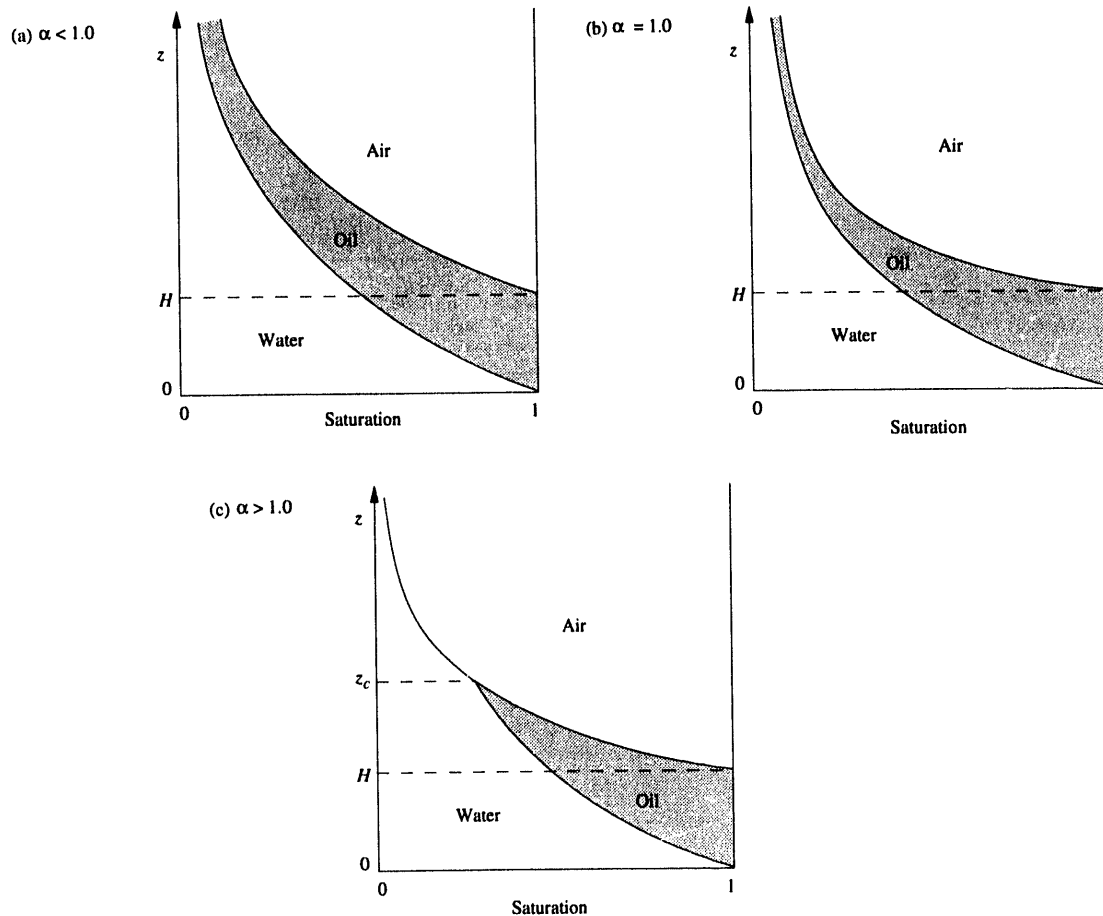


Figure 9: The distributions of water, oil and gas in vertical equilibrium. (a) for  $\alpha < 1$ ; (b) for  $\alpha = 1$ ; and (c) for  $\alpha > 1$ .

sum of Eqs. 9 and 10). The gas/water interfaces will be polluted with an oil film, giving a lowered effective gas/water surface tension and an effective spreading coefficient that is approximately zero [1, 27]. For continuity of the water phase at  $z = z_c$  the effective gas/water surface tension must be  $\gamma_{ow} + \gamma_{go}$ .

### How much oil can be trapped?

If gas displaces connected oil, there is no mechanism for the oil to become trapped and the oil saturation above  $z_c$  will be zero. If gas displaces trapped oil, such as waterflood residual oil in a reservoir, or immobile product just below the water table, oil can remain trapped if it has not been directly contacted by gas. This interpretation is consistent with sand column experiments which showed better recoveries for gravity drainage from continuous oil than for drainage of hitherto residual oil [16].

In this section we will consider gravity drainage of previously discontinuous oil. An indication of the amount of oil that can remain trapped is the water saturation at  $z_c$ . Trapped oil at  $z = z_c$  is contained in ganglia completely surrounded by water that has not been displaced by gas. At

heights above and below  $z_c$  less oil will be trapped. Above  $z_c$ , the water saturation is lower and more oil will have been contacted by gas. Below  $z_c$  the mobile oil will have reconnected previously trapped ganglia. If we know the three phase capillary pressures, we can calculate the oil and water saturations. One possible parameterization for the capillary pressure function  $J$  is [5]

$$J(S_w) = J^* S^{-1/\lambda}, \quad (19)$$

where  $J^*$  represents the threshold entry curvature [7],  $S$  is the wetting phase saturation and  $\lambda$  is a constant that depends on the pore structure of the medium and is generally in the range 0.2-1.0 [18]. Other expressions for the capillary pressure have been proposed [25, 30]. The capillary pressure we use has no irreducible or residual water saturation [18]. We could allow an irreducible water saturation, but we do assume that all the oil filled pores can be accessed by gas.

We use Eqs. 9, 11, 16 and 19 to find the water saturation as a function of height

$$S_w = \left( 1 + \frac{z(\rho_o - \rho_g)g}{\alpha J^* \gamma_{go}} \right)^{-\lambda}. \quad (20)$$

and at  $z = z_c$ , from Eq. 18

$$S_w(z_c) = \left( 1 + \frac{H(\rho_o - \rho_g)g}{(\alpha - 1)J^* \gamma_{go}} \right)^{-\lambda}. \quad (21)$$

If we increase  $H$ , the water saturation at  $z_c$  decreases, as illustrated in Fig. 10. This means that the trapped oil saturation at  $z_c$  decreases and the gravity drainage process is more efficient. If we take typical values for a polluted sandy soil:  $H = 0.1$  m,  $J^* = 10^4$  m<sup>-1</sup>,  $\alpha = 4$ ,  $\lambda = 1$ ,  $\rho_w - \rho_g = 10^3$  kgm<sup>-3</sup>,  $\rho_o - \rho_g = 700$  kgm<sup>-3</sup> and  $\gamma_{go} = 0.02$  Nm<sup>-1</sup>, we find  $S_w = 0.47$ , which could allow some oil to be trapped. However, if the pore size distribution is uniform, very little oil remains trapped, even for small values of  $H$ , as demonstrated in sand column experiments [16]. In contrast, a large oil bank in a water-wet reservoir, with the same values as above, except  $J^* = 10^5$  m<sup>-1</sup> and  $H = 100$  m, gives  $S_w$  as less than 1%. The residual oil saturation at  $z_c$  must therefore be much less than 1%. Oil is only trapped if we have a mixed-wet or oil-wet system.

If we have a nonspreading system, three phase contact lines between the phases are stable, oil films and layers do not form and oil can remain trapped. The recovery from gravity drainage will be lower than for systems with  $C_s > 0$  with the same value of  $\alpha$ .

## Experimental confirmation

Several investigators have performed gravity drainage experiments, where gas displaces water and residual oil, or oil and residual water, under gravity [4, 6, 10, 16, 17, 31] and have shown that final oil saturations as low as 1% are possible. These very good recoveries have been explained by the drainage of oil layers between the gas and water [14, 15, 24, 23, 28]. It has been shown that lower final oil saturations are seen for systems with a positive spreading coefficient than for nonspreading oils [15, 24, 31]. However, none of these authors made quantitative predictions of the variation of recovery with fluid properties.

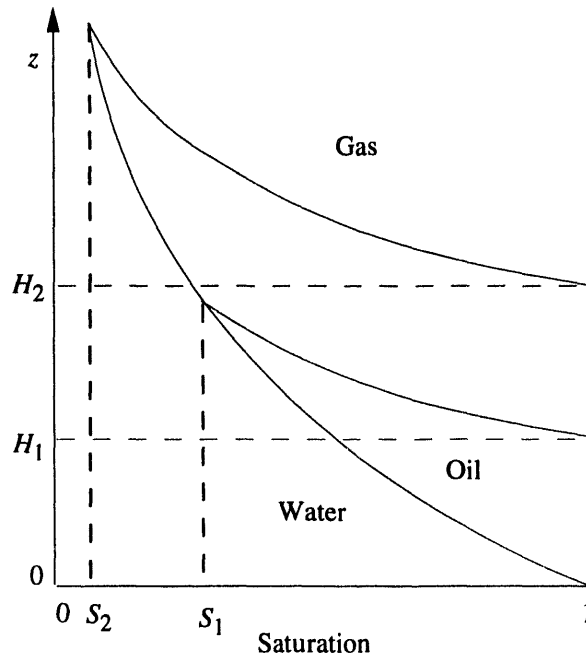


Figure 10: A schematic of water saturation variation with the increases in the height of oil bank.

We performed experiments in sand columns of two heights: a long column of 97.5 cm, and a short column of 47 cm. Both columns had a diameter of 2 cm. They were filled with a clean, well-sorted sand with a mean grain diameter of approximately  $0.3 \mu\text{m}$ , a permeability of 48 D and porosity of 0.28.

The sand column was first fully saturated with water. The top and bottom valves at the end of the column were then both opened to allow the invasion of air and the free drainage of water. We waited at least 24 hours until no further water was produced.  $30 \text{ cm}^3$  of oil was then slowly poured into the top of the column to represent the migration of pollutant towards the water table. Oil accumulated at the bottom of the column and was allowed to drain out freely. Periodically, air at just above atmospheric pressure was pumped into the top of the column to displace the oil bank. This exercise stopped when there was no further production of fluids. No further oil was recovered after two weeks of drainage.

For a nonspreading mineral oil (Drakeol 5), we found that  $14 \text{ cm}^3$  remained in the long column and  $9 \text{ cm}^3$  remained in the short column. Zhou and Blunt [32] conducted the experiment described here for spreading systems with various values of  $\alpha$ . By using Corey type capillary pressures, Eq. 19, the amount of oil left in the columns could be matched using  $\lambda = 0.92$ , a value previously measured on a well-sorted sand by Lenhard and Parker [18].

Fig. 11 plots the results for both the spreading and nonspreading oils. There is little change in oil saturation with  $\alpha$  for the short column. This is because the critical height  $z_c$  is above the top of the column for most of the experiments, and thus it is difficult to distinguish between  $\alpha < 1$ ,  $\alpha > 1$ , spreading and nonspreading systems. For the long column, however, the average saturation at the end of the experiment decreases from approximately 16% for  $\alpha = 0.47$  to 8% for  $\alpha = 4.0$ . The difference in recovery for the two columns represents the amount of oil

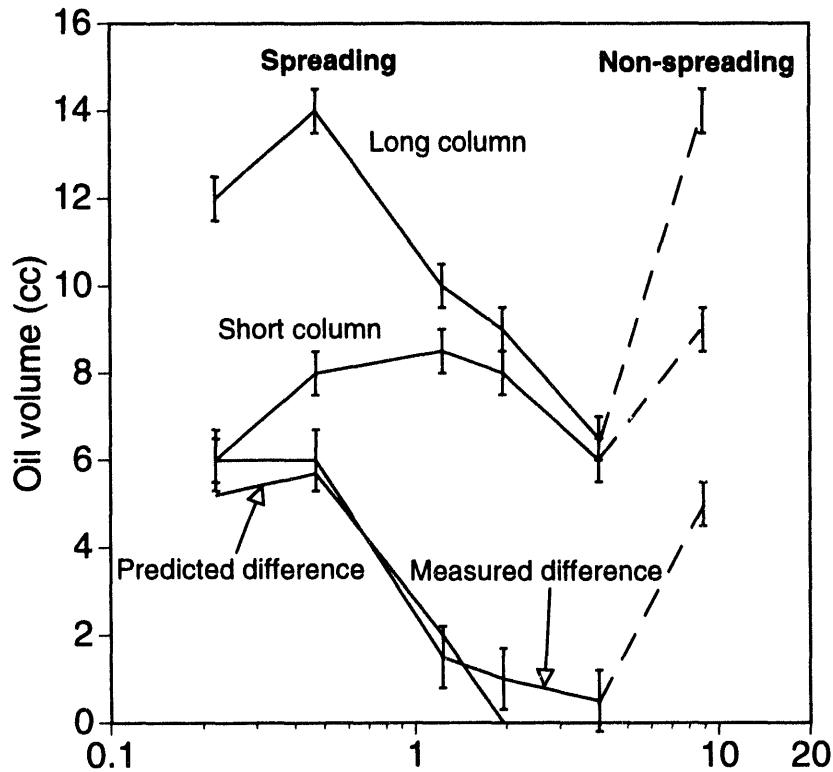


Figure 11: The amount of oil remaining in the sand columns as a function of  $\alpha$ .

remaining in the upper portion of the long column which varies from 14 l for  $\alpha = 0.47$  to  $1 \pm 1\%$  for  $\alpha = 4.0$ . For a spreading system, the final oil saturation well above the oil/water contact changes by a factor of twelve with  $\alpha$ . The oil remaining can be predicted successfully, as shown in Fig. 11. For large  $\alpha$  the amount left is zero to within experimental error. The nonspreading oil (the points to the right in Fig. 11) gives a poor recovery, even though it has a large value of  $\alpha$ , because in this case oil can be trapped.

## Discussion

The critical parameter that determines oil recovery by gravity drainage for a spreading system is  $\alpha$ , which is a property of the fluid system alone and independent of the porous medium, as long as it is water-wet. For most fluids  $\alpha > 1$ , which means that above a critical height the residual oil saturation can be zero. However, if surfactant flooding is used to displace oil in the presence of gas, this will dramatically decrease  $\gamma_{ow}$ , and  $\alpha$  will be less than 1. This will mean that in vertical equilibrium, appreciable quantities of oil can be retained above the oil/water contact. The recovery of oil from gravity drainage is most efficient for large  $\alpha$ , which can be achieved by lowering the gas/oil surface tension. In oil reservoirs, the natural gas may be almost miscible with the oil, leading to very low values of  $\gamma_{go}/(\rho_o - \rho_g)$  and an extremely high oil recovery.

### 3.6 Conclusions

The mechanism of gravity drainage is transport through thick oil layers sandwiched between water and gas, which occupy the crevices of the pore space. These layers form spontaneously if the spreading coefficient is positive. In the experiments we performed, nonspreading systems did not form oil layers and gave poorer recoveries.

The distribution of oil, water and gas in vertical equilibrium for a spreading system is controlled by the parameter  $\alpha$ , Eq. 16. Typically  $\alpha > 1$ , and there is a finite height above which the oil saturation can be zero, apart from thin molecular films. This height is a function only of the fluid densities and surface tensions and is independent of the soil or rock type. For  $\alpha < 1$ , which is seen for surfactant floods, a large quantity of oil can be contained above the oil bank.

### References

- [1] Adamson, A. A.: *Physical Chemistry of Surfaces*, John Wiley & Sons, Inc., New York (1990).
- [2] Bear, J.: *Dynamics of Fluids in Porous Media*, American Elsevier, New York (1972).
- [3] Blunt, M. J., Zhou, D. and Fenwick, D.: "Three Phase Flow and Gravity Drainage in Porous Media," unpublished (1994).
- [4] Blunt, M.J., Fenwick, D. and Zhou, D.: "What Determines Residual Oil Saturation in Three Phase Flow?," paper SPE 27816 presented at the 1994 Ninth Symposium on Improved Oil Recovery, Tulsa, OK, April.
- [5] Brooks, R. H. and Corey, A. T.: "Properties of Porous Media Affecting Fluid Flow," *Irrigation and Drainage Division of the ASCE Journal* (1966) **92**, 61-88.
- [6] Chatzis, I., Kantzas, A. and Dullien, F. A. L.: "On the Investigation of Gravity-Assisted Inert Gas Injection Using Micromodels, Long Berea Sandstone Cores, and Computer-Assisted Tomography," paper SPE 18284 presented at the 1988 SPE Annual Technical Conference and Exhibition, Houston, TX, October 2-5.
- [7] Corey, A. T.: *Mechanics of Immiscible Fluids in Porous Media*, Water Resources Publications, Littleton, CO (1986) 253.
- [8] Derjaguin, B. v. and Kussakov, M. M.: "Anomalous Properties of Thin Polymolecular Films V," *Acta Physicochim URSS* (1939) 25.
- [9] Dullien, F. A. L.: *Porous Media, Fluid Transport and Pore Structure*, Academic Press, San Diego (1992).
- [10] Dumoré, J.M. and Schols, R.S.: "Drainage Capillary Pressure Functions and the Influence of Connate Water," *Soc. Pet. Eng. J.* (1974) 437-444.

- [11] Gibbs, J. W.: *The Collected Works of J. Willard Gibbs*, Longmans, Green, New York (1928).
- [12] Hagedorn, K.: *Component Partitioning in CO<sub>2</sub>/Crude Oil Mixtures*, PhD dissertation, Stanford University (1992).
- [13] Hirasaki, G. J.: "Modeling the Effects of Trapping and Water Alternate Gas (WAG) Injection on Tertiary Miscible Displacements," paper SPE 17367 presented at the 1988 Sixth Symposium on Enhanced Oil Recovery, Tulsa, OK, April.
- [14] Kalaydjian, F. J.-M.: "Performance and Analysis of Three-Phase Capillary Pressure Curves for Drainage and Imbibition in Porous Media," paper SPE 24878 presented at the 1992 SPE Technical Conference and Exhibition, Washington, D.C.
- [15] Kalaydjian, F. J.-M., Moulu, J.-C., Vizika, O. and Munkerud, P. K.: "Three-Phase Flow in Water-Wet Porous Media: Determination of Gas/Oil Relative Permeabilities under Various Spreading Conditions," paper SPE 26671 presented at the 1993 SPE Technical Conference and Exhibition, Houston, TX.
- [16] Kantzas, A., Chatzis, I. and Dullien, F. A. L.: "Enhanced Oil Recovery by Inert Gas Injection," paper SPE 17379 presented at the 1988 Sixth Symposium on Enhanced Oil Recovery, Tulsa, OK, April.
- [17] Kantzas, A., Chatzis, I. and Dullien, F. A. L.: "Mechanisms of Capillary Displacement of Residual Oil by Gravity-Assisted Inert Gas Injection," paper SPE 17506 presented at the 1988 Rocky Mountain Regional Meeting, Casper, WY.
- [18] Lenhard, R. J. and Parker, J. C.: "Estimation of Free Hydrocarbon Volume from Fluid Levels in Monitoring Wells," *Ground Water* (January-February 1990) **28**, No. 1, 57-67.
- [19] Leverett, M. C.: "Capillary Behavior in Porous Solids," *Trans., AIME* (1941) **142**, 152-169.
- [20] Mohanty, K.K., Davis, H.T. and Scriven, L.E.: "Physics of Oil Entrapment in Water-Wet Rock," *SPE Reservoir Engineering* (February 1987) 113-128.
- [21] Muskat, M.: *Principles of Oil Production*, McGraw Hill, Boston (1949).
- [22] Oren, P. E. and Pinczewski, W. V.: "The Effects of Film Flow on Mobilization of Waterflood Residual Oil by Immiscible Gas Flooding," (May 21-23 1991) 6th European IOR Symposium, Stavanger, Norway.
- [23] Oren, P. E. and Pinczewski, W. V.: "The Effect of Wettability and Spreading Coefficients on the Recovery of Waterflood Residual Oil by Miscible Gasflooding," paper SPE 24881 presented at the 1992 SPE Technical Conference and Exhibition, Washington, D.C.
- [24] Oren, P. E., Billiotte, J. and Pinczewski, W. V.: "Mobilization of Waterflood Residual Oil by Gas Injection for Water-Wet Conditions," *SPE Formation Evaluation* (March 1992) 70-78.

- [25] Parker, J. C., Lenhard, R. J. and Koppusamy, T.: "A Parametric Model for Constitutive Properties Governing Multiphase Flow in Porous Media," *Water Resources Research* (1987) **23**, 618-624.
- [26] Roof, J.G.: "Snap-Off of Oil Droplets in Water-Wet Pores," *Soc. Pet. Eng. J.* (March 1970) 85-90.
- [27] Rowlinson, J. S.: *Molecular Theory of Capillarity*, Clarendon Press, Oxford (1989).
- [28] Soll, W. E., Celia, M. A. and Wilson, J. L.: "Micromodel Studies of Three-Fluid Porous Media Systems: Pore-Scale Processes Relating to Capillary Pressure-Saturation Relationships," *Water Resources Research* (1993) **29**, No. 9, 2963-2974.
- [29] Thiele, M. R., Blunt, M. J. and Orr, Jr. F. M.: "Predicting Multicomponent, Multiphase Flow in Heterogeneous Systems using Streamtubes," (June 1994) Fourth European Conference on the Mathematics of Oil Recovery, Norway.
- [30] van Genuchten, M. T.: "A Closed-Form Equation for Predicting the Hydraulic Conductivity of Unsaturated Soils," *Soil Science Society of American Journal* (1980) **44**, 892-898.
- [31] Vizika, O.: "Effect of the Spreading Coefficient on the Efficiency of Oil Recovery with Gravity Drainage," Presented at the Symposium on Enhanced Oil Recovery, presented before the Division of Petroleum Chemistry, Inc., Denver, Colorado (1993).
- [32] Zhou, D. and Blunt, M. J.: "Distribution of Light Non-aqueous Phase Liquid in Subsurface," unpublished (1994).
- [33] Zhou, D., Fayers, F.J. and Orr, F.M., Jr.: "Scaling Multiphase Flow in Simple Heterogeneous Porous Media," paper SPE 27816 presented at the 1994 Ninth Symposium on Improved Oil Recovery, Tulsa, OK, April.

**DATE  
FILMED**

10 / 5 / 94

**END**

